

Optical properties of carbon nanotubes

Xiangang Wan and Jinming Dong

*National Laboratory of Solid State Microstructures, Nanjing University, Nanjing 210008, People's Republic of China
and Center for Advanced Studies in Science and Technology of Microstructures, Nanjing 210093, People's Republic of China*

D. Y. Xing

Department of Physics, Nanjing University, Nanjing 210008, People's Republic of China

(Received 9 December 1997; revised manuscript received 26 February 1998)

Using the extended Hubbard model and sum-over-state method, we have calculated the linear polarizability α and the third-order nonlinear polarizability γ for carbon nanotubes with finite lengths. We find that the chiral symmetry of nanotubes with finite length has a great effect on their optical properties. For example, the finite length (n,m) tubes with $n-m$ being not a multiple of 3, will have smaller α and much smaller γ values than other finite length tubes. [S0163-1829(98)01832-3]

Carbon nanotubes have been investigated intensively as a different form of one-dimensional material¹⁻⁴. Each single-layer nanotube can be regarded as a rolled-up graphite sheet in the cylindrical form. The geometrical structure of the nanotube is uniquely determined by its circumference vector, $\mathbf{R} = n_1 \mathbf{a}_1 + n_2 \mathbf{a}_2$, where \mathbf{a}_1 and \mathbf{a}_2 are lattice translation vectors on the graphite sheet, and n_1 and n_2 are integers.⁵ The pair number (n_1, n_2) defines the radius and chirality of each tube. As a result of their seamless cylindrical graphitic structure, nanotubes are predicted to have interesting mechanical properties, in particular, high stiffness and axial strength.⁶ Theoretical studies have shown that a carbon nanotube is either metallic or semiconducting, depending on its diameter and geometric symmetry.⁷ Experiments also indicate that the nanotube can be used as an atomic-scale field emitter and as pinning material in high- T_c superconductors.^{8,9} The nanotubes were usually treated as periodic infinite one-dimensional crystals in the aforementioned theoretical studies. But actual nanotubes have finite lengths, so it is interesting to study physical properties of the carbon nanotubes with finite lengths.

The nanotubes possess a large number of conjugated π electrons and are entirely composed of carbon atoms. They do not have any residual infrared absorption due to overtones of C-H stretching vibrations that organic molecules usually have. In this paper, we investigate how the finite length and the chiral symmetry of a nanotube influence its optical properties.

The tips of the nanotubes are very complicated. Some nanotubes have closed caps, and others do not. We call the nanotube with a cap a "capped nanotube," and that without a cap an "uncapped nanotube." We cut the nanotube perpendicular to its axis, and make the carbon atoms at the open end have two σ bonds to connect with other carbon atoms. The exact geometry of the open end of the nanotube is very complicated, and we find that they are almost not relevant to the optical properties of nanotube, in particular when the nanotube is long. For simplicity, we label the uncapped (n,m) nanotube with k carbon atoms as $(n,m)k$. In this paper, we study only uncapped nanotubes. The γ values of C_{60} calculated with the free-electron model are in agreement

with the experiment, while the linear absorption spectra are not in agreement with experiments. If Coulomb interactions are taken into account, the absorption spectra are in overall agreement with the experiment, although the magnitude of the γ decreases by a factor of about 0.1.^{10,11} For other fullerenes, the effect of Coulomb interaction is not known. So it is interesting to study whether or not Coulomb interaction also has a great effect on the electronic structure and optical properties of the nanotubes. Therefore, in this paper, we will use the extended Hubbard model¹² to calculate electronic structures of the nanotubes, and then use the sum-over-states (SOS) approach to calculate their linear polarizability α and the third-order polarizability γ .¹³

For the nanotubes, the model Hamiltonian can be written as

$$\begin{aligned}
 H = & \sum_{\langle ij \rangle, s} [-t_0 - \alpha(|r_i - r_j| - d_0)] (c_{i,s}^\dagger c_{j,s} + \text{H.c.}) \\
 & + \frac{K}{2} \sum_{\langle ij \rangle} (|r_i - r_j| - d_0)^2 + U \sum_i c_{i,\uparrow}^\dagger c_{i,\uparrow} c_{i,\downarrow}^\dagger c_{i,\downarrow} \\
 & + V \sum_{\langle ij \rangle} \sum_s \sum_{s'} c_{i,s}^\dagger c_{i,s} c_{j,s'}^\dagger c_{j,s'}, \quad (1)
 \end{aligned}$$

where we have assumed that the bonds at the end caps of the nanotubes are hydrogenized, and so there is not dangling bonds in our calculation. t_0 is the hopping constant, α is the electron-phonon coupling constant. The operator $c_{i,s}(c_{i,s}^\dagger)$ annihilates (creates) a π electron at the i th carbon atom with spin s , r_i is the position of the i th carbon atom, d_0 is the average separation between two adjacent atoms. K is the spring constant between the adjacent units, U is the usual on-site Coulomb repulsion strength for a carbon atom, V is the Coulomb interaction between the nearest-neighbor carbon atoms, and the sum $\langle i, j \rangle$ is taken over the nearest-neighbor pairs. Using the Hartree-Fock approximation, Eq. (1) is transformed into

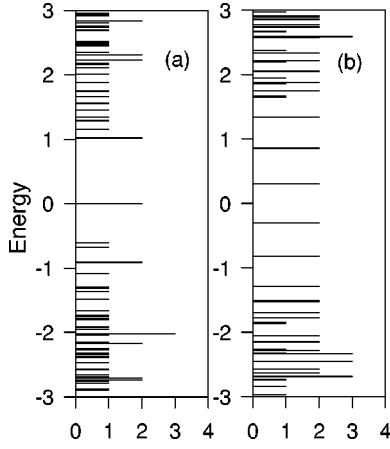


FIG. 1. Energy-level structure around the HOMO and LUMO of nanotubes. The line length is proportional to the degeneracy of the energy level. The shortest line is for undegenerate levels. (a) (6,4)200, (b) (6,3)198.

$$\begin{aligned}
H = & \sum_{\langle ij \rangle, s} [-t_0 - \alpha(|r_i - r_j| - d_0)](c_{i,s}^\dagger c_{j,s} + \text{H.c.}) \\
& + \frac{K}{2} \sum_{\langle ij \rangle} (|r_i - r_j| - d_0)^2 + U \sum_i \left(\sum_s \rho_{i,s} c_{i,s}^+ c_{i,s} \right. \\
& \left. - \rho_{i,\uparrow} \rho_{i,\downarrow} \right) + V \sum_{\langle ij \rangle} \sum_s \left(\sum_{s'} \rho_{j,s'} c_{i,s}^\dagger c_{i,s} \right. \\
& \left. - \rho_{i,s} \sum_{s'} \rho_{j,s'} - \tau_{ij,s} c_{i,s}^\dagger c_{j,s} + \tau_{ij,s}^2 \right), \quad (2)
\end{aligned}$$

where $\rho_{i,s} = \langle c_{i,s}^\dagger c_{i,s} \rangle$ is the electron density at the i th site with spin s , and $\tau_{ij,s} = \langle c_{i,s}^\dagger c_{j,s} \rangle$ is the bond order parameter.

Equation (1) is solved by the adiabatic approximation for phonons. The Schrödinger equation for the π electron is

$$\begin{aligned}
\varepsilon_k Z_{k,s}(i) = & \sum_{\langle ij \rangle} [-t_0 - \alpha(|r_i - r_j| - d_0) - V \tau_{ij,s}] Z_{k,s}(j) \\
& + \left[U \rho_{i,s} + V \sum_{j,s'} \rho_{j,s'} \right] Z_{k,s}(i), \quad (3)
\end{aligned}$$

where ε_k and $Z_{k,s}$ are the eigenvalue and eigenfunction, respectively. The self-consistent equation for the lattice is

$$\begin{aligned}
(|r_i - r_j| - d_0) = & -\frac{2\alpha}{K} \sum_{k,s} \sum' Z_{k,s}(i) Z_{k,s}(j) \\
& + \frac{2\alpha}{K} \frac{1}{N} \sum_{\langle ml \rangle} \sum_{k,s} \sum' Z_{k,s}(m) Z_{k,s}(l), \quad (4)
\end{aligned}$$

where the prime in the summation indicates a sum over occupied states, the second term is due to the constraint $\sum_{\langle ij \rangle} (|r_i - r_j| - d_0) = 0$, and N is the number of π bonds. From Eqs. (3) and (4), we can get ε_k and $Z_{k,s}$ self-consistently.

Within the independent electron approximation and sum-over-states approach, the linear polarizability $\alpha(\omega)$ is expressed as

$$\alpha(\omega) = 2 \sum_{\substack{n \in \text{occ.} \\ p \in \text{unocc.}}} \mu_{np} \mu_{pn} \left(\frac{1}{\epsilon_{pn} - \omega} + \frac{1}{\epsilon_{pn} + \omega} \right), \quad (5)$$

and the third-order polarizability γ can be expressed as follows:

$$\gamma(-3\omega; \omega, \omega, \omega) = \gamma_1 + \gamma_2 + \gamma_3 + \gamma_4 + \gamma_5, \quad (6)$$

$$\gamma_1(-3\omega; \omega, \omega, \omega) = 2 \sum_{\substack{l, m, n \in \text{occ.} \\ p \in \text{unocc.}}} \mu_{pn} \mu_{nm} \mu_{ml} \mu_{lp} S_1(\omega),$$

$$\begin{aligned}
S_1(\omega) = & \frac{1}{(\epsilon_{pn} - 3\omega)(\epsilon_{pm} - 2\omega)(\epsilon_{pl} - \omega)} \\
& + \frac{1}{(\epsilon_{pn} + \omega)(\epsilon_{pm} + 2\omega)(\epsilon_{pl} - \omega)} \\
& + \frac{1}{(\epsilon_{pn} + \omega)(\epsilon_{pm} - 2\omega)(\epsilon_{pl} - \omega)} \\
& + \frac{1}{(\epsilon_{pn} + \omega)(\epsilon_{pm} + 2\omega)(\epsilon_{pl} + 3\omega)}.
\end{aligned}$$

The forms of γ_2 , γ_3 , γ_4 , and γ_5 are similar to γ_1 .¹³

In the above formula, $\epsilon_{np} = \epsilon_n - \epsilon_p$, and μ_{nm} is the dipole transition matrix elements between the one-electron state $Z_{n,s}$ and $Z_{m,s}$, which is given by

$$\langle n | \mu_\alpha | m \rangle = \sum_{j,s} Z_{n,s}^*(j) (-e \alpha_j) Z_{m,s}(j). \quad (7)$$

Equations (1)–(7) are our basic equations used to calculate $\alpha(\omega)$ and $\gamma(-3\omega; \omega, \omega, \omega)$ for nanotubes.

In our numerical calculation, the Coulomb interaction parameters are taken to be $U = 2V = t_0$, and other parameters are taken as $t_0 = 1.8$ eV, $\alpha = 3.5$ eV/Å, $K = 30$ eV/Å² and $d_0 = 1.42$ Å, which have been successfully used in C₆₀.¹⁴ Based upon a periodic boundary condition along the nanotube axis, electronic structure of the infinite length nanotubes has first been calculated, and obtained results are in agreement with other theoretical results, i.e., a (n, m) tube is metal or semiconductor, depending on whether or not its $n-m$ is a multiple of 3. We then have calculated electronic structures of the uncapped nanotubes, and obtained electronic energy band structures for (6,4)200 and (6,3)198 nanotubes are shown in Figs. 1(a) and 1(b), respectively. From Fig. 1, it can be seen that the rotational symmetries of nanotubes have a great influence upon their electronic structures. The tubes (6,3)198 and (6,4)200 have C_3 and C_2 symmetry, respectively. Since the former has higher symmetry, its energy levels have higher degeneracies than the latter. The energy gap (E_g) of (6,3)198 is not zero, but for (6,4)200, its highest occupied molecular orbital (HOMO) and its lowest unoccupied molecular orbital (LUMO) are degenerate. We increase lengths of both the (6,3) and (6,4) tubes and find that their electronic structures are similar to those of (6,3)198 and (6,4)200, respectively. For the uncapped (6,3) tubes, their E_g is not zero, and the intervals between two neighboring energy levels near the Fermi surface are similar. For the uncapped (6,4) tubes, their E_g is zero, and the energy differ-

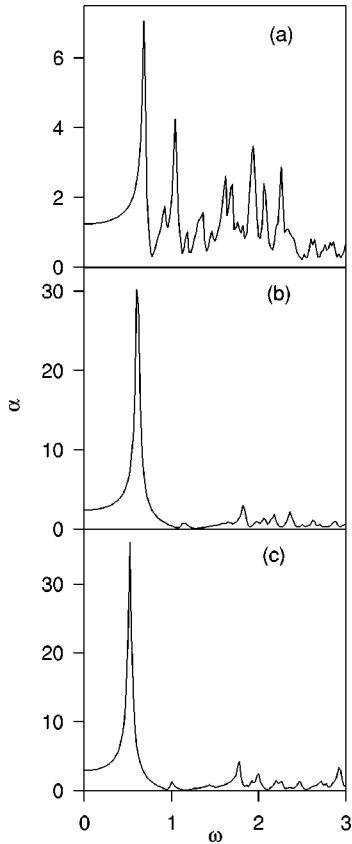


FIG. 2. The linear polarizability α spectra for nanotubes (in 10^3 \AA^3). The unit of x coordinate is eV. (a) (6,4)200, (b) (6,3)198, (c) same (6,3)198, but for free electron case.

ence between the HOMO and the next highest occupied level is much bigger than the interval of other two neighboring energy levels. Similarly, the energy difference between the LUMO and the next lowest unoccupied level is also much bigger than the interval of other two neighboring energy levels. This means that the uncapped (6,3) and (6,4) tubes are semiconductor and metal, respectively. Oppositely, infinite length (6,3) and (6,4) tubes are metal and semiconductor, respectively. The difference between the electronic structures of infinite and finite length nanotubes comes from the periodic boundary condition along the axis of the nanotube with infinite length. On the other hand, the rotational symmetry of the finite length tubes has also an important effect on the differences between the electronic structures of (6,3) and (6,4) tubes. We have also calculated other uncapped tubes. It seems that for an uncapped (n,m) tube, if its $n-m$ is not a multiple of 3, its electronic structure is similar to that of the uncapped (6,4) tube.

The linear polarizability α of a nanotube is calculated, based upon their electronic structures obtained above. Because the ratios between the different components of α are not known, its spatial averages are defined as $\alpha = \frac{1}{3}(\alpha_{xx} + \alpha_{yy} + \alpha_{zz})$. Here, the z axis is taken along the nanotube axis. Because a nanotube length is much larger than its diameter, its μ_z is much larger than its μ_x and μ_y , making the α value increase with increasing of the atom number in the nanotube. For most of uncapped nanotubes, the transition between their HOMO and LUMO is allowed, and the value of $\langle \text{HOMO} | \mu_z | \text{LUMO} \rangle$ is much bigger than other terms,

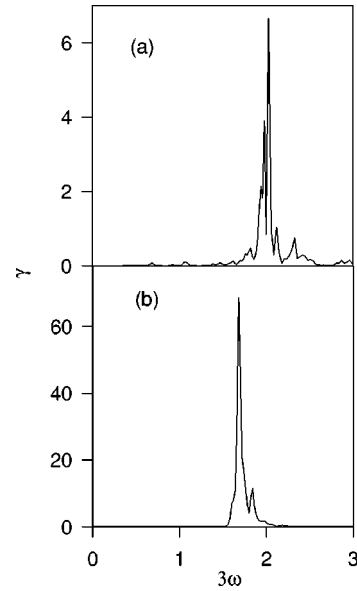


FIG. 3. The third-order polarizability γ spectra for nanotubes (in 10^{-29} esu). The unit of the x coordinate is eV. (a) (6,4)200, (b) (6,3)198.

making the transition between HOMO and LUMO very important. The α spectra of (6,3)198 and (6,4)200 are shown in Fig. 2, from which it can be seen that although (6,3)198 and (6,4)200 have similar μ values, their α spectra are greatly different. For (6,3)198, the first peak in the α spectra is the highest peak with height of $30.1 \times 10^3 \text{ \AA}^3$, which is much bigger than the values of other peaks. However, for (6,4)200, its value of highest peak is only $7.1 \times 10^3 \text{ \AA}^3$, which is four times smaller than that of (6,3)198. It is because the first peak of (6,3)198 is produced by the transition between HOMO and LUMO, and its $\langle \text{HOMO} | \mu_z | \text{LUMO} \rangle = 5.56$ is the biggest term in its dipole matrix elements. On the other hand, for (6,4)200, its HOMO and LUMO are degenerate, and so, its highest peak is produced by a transition between the 98th and 101st energy levels, but its $\langle 98 | \mu_z | 101 \rangle = 2.78$, causing the corresponding α value to be smaller than that of (6,3)198. The difference between α spectra of (6,3)198 and (6,4)200 tubes mainly comes from the difference in their electronic structures. Since most of finite-length (n,m) tubes with $n-m$ being not a multiple of 3 have similar electronic structures to those of finite length (6,4) tube, all of them will have small α values. For example, the uncapped (7,3) tubes have smaller α values. Its static and the biggest α values are $1.1 \times 10^3 \text{ \AA}^3$ and $6.1 \times 10^3 \text{ \AA}^3$, respectively. On the other hand, the static values of (6,3)198, (5,5)200, (9,0)198, and (6,4)200 are 2.4, 1.8, 2.4, and $1.2 \times 10^3 \text{ \AA}^3$, respectively. The biggest α values of (5,5)200 and (9,0)198 are 18.1 and $25.5 \times 10^3 \text{ \AA}^3$, respectively. So, we can conclude that the finite length tubes with $n-m$ being a multiple of 3 have bigger α values than other finite length tubes.

We have also investigated the third-order nonlinear polarizability γ of nanotube. A spatial average of γ is given as $\gamma = \frac{1}{5}[\gamma_{xxxx} + \gamma_{yyyy} + \gamma_{zzzz} + 2(\gamma_{xxyy} + \gamma_{yyzz} + \gamma_{zzxx})]$. The dispersion curves of the third-order polarizability γ of (6,3)198 and (6,4)200 have been shown in Fig. 3, from which it can be seen that the rotational symmetry also has great effect on the γ spectra. Both the highest peaks in the γ

TABLE I. Heights of the highest peaks in the γ spectra of finite length nanotubes.

	(7,3)200	(6,4)200	(6,3)198	(5,5)200	(9,0)198
$\gamma(10^{-29}$ esu)	0.6	6.4	68.6	63.5	69.7

spectra of (6,3)198 and (6,4)200 are three resonance enhancement peaks (i.e., single-photon, two-photon, and three-photon resonance enhancement peak). But, the height of the highest peak of (6,3)198 is about ten times bigger than that of (6,4)200. The reason is that for uncapped (6,3) tube, the intervals between two neighboring energy levels near the Fermi surface are similar, making the γ values increase. So, although (6,3)198 and (6,4)200 tubes have almost the same size, the uncapped (6,3) tubes have much bigger γ values than those of uncapped (6,4) tubes. Thus, we can also conclude that the finite length tubes with $(n-m)/3$ being an integer have much larger γ values than other finite length tubes. We listed the highest γ values for some finite length nanotubes in Table I. From Table I, we can see that the uncapped (7,3) tube has the smallest γ value, and the uncapped (9,0) tube has the biggest γ value, which is in agreement with the aforementioned discussion.

In addition to (5,5), (9,0), (6,3), (6,4), and (7,3) tubes, we have also calculated other finite length tubes with different symmetries, and found that (4,4), (6,6), (7,7), and (12,0) tubes have bigger α and γ values, but oppositely, the α and γ values of (8,0), (14,0), and (7,1) tubes are smaller. On the other hand, we have also increased the tube lengths, and found that the α values of (6,3)1998 are also much larger than those of (6,4)2000. Thus we can conclude that our conclusions obtained above are correct for most finite length tubes.

We have also investigated the free-electron case in order to see clearly the effect of Coulomb interaction, and shown

the α spectra of (6,3)198 in Fig. 2(c). It has been found that Coulomb interactions among π electrons increase the energy difference between two neighboring energy levels. From Fig. 2(c), we can find that the Coulomb interactions will decrease the α value of the tube and make peak positions in α spectra go to the right, i.e., to higher frequencies. The influence of Coulomb interaction on γ spectra is similar to that on α spectra, but the former is bigger. However, compared with the chiral symmetry of tubes, the Coulomb interaction has been found to have a much smaller effect on the electronic structure and optical properties of the finite length tubes. So, for free-electron case, the conclusions obtained above about α and γ spectra are still correct. The σ - π band mixing effect due to the curvature of the nanotubes is small.¹⁵ This effect has been neglected in our calculation, so our conclusion is qualitatively correct.

In conclusion, we find that the finite length (n,m) tubes with $n-m$ being not a multiple of 3 will have smaller α and γ values, no matter whether or not Coulomb interaction is included. It should be indicated that we assume the bonds at the end caps of the nanotubes are hydrogenized and so the effect of the dangling bonds has not included in our calculation.

So, by analyzing only their electronic structure, we can know the optical properties of the uncapped nanotubes. On the other hand, if we know their optical properties, we can also deduce some of their electronic properties and geometrical structures. We hope that obtained results in this paper will be helpful to distinguish different nanotubes by their optical properties.

This work was supported by the Natural Science Foundation of China under Grant No. 19674027, and the NSF of Jiangsu Prov. through Grant No. BK 97022. We also acknowledge support from the Climbing Project of China through Grant No. 85-6 NMS (Nanomaterials Science).

¹S. Iijima, Nature (London) **354**, 56 (1991); S. Iijima and T. Ichihashi, *ibid.* **363**, 603 (1993).

²S. Iijima, T. Ichihashi, and Y. Ando, Nature (London) **356**, 776 (1992).

³L. X. Benedict, S. G. Louie, and M. L. Cohen, Phys. Rev. B **52**, 8541 (1995).

⁴T. W. Ebbesen *et al.*, Nature (London) **382**, 54 (1996); A. Thess *et al.*, *ibid.* **273**, 483 (1996); H. Dai, E. W. Wong, and M. Lieber, *ibid.* **272**, 523 (1996).

⁵C. T. White, D. H. Robertson, and J. M. Mintimire, Phys. Rev. B **47**, 5485 (1993); R. A. Jishi, M. S. Dresselhaus, and G. Dresselhaus, *ibid.* **47**, 16 671 (1993); R. A. Jishi, L. Venkataraman, M. S. Dresselhaus, and G. Dresselhaus, *ibid.* **51**, 11 176 (1995).

⁶M. M. J. Treacy, T. W. Ebbesen, and J. M. Gibson, Nature (London) **381**, 678 (1996).

⁷N. Hamada, S. Sawada, and A. Oshiyama, Phys. Rev. Lett. **68**,

1579 (1992); R. Saito, M. Fujita, G. Dresselhaus, and M. S. Dresselhaus, Appl. Phys. Lett. **60**, 2204 (1992).

⁸A. G. Rinzler *et al.*, Science **269**, 1550 (1995); W. A. De Heer, A. Chatelain, and D. Ugarte, *ibid.* **270**, 1179 (1995).

⁹K. Fossheim *et al.*, Physica C **248**, 195 (1995).

¹⁰K. Harigaya and S. Abe, Phys. Rev. B **49**, 16 746 (1994).

¹¹K. Harigaya and S. Abe, J. Lumin. **60&61**, 380 (1994).

¹²R. J. Cohen and A. J. Glick, Phys. Rev. B **40**, 8010 (1989); G. W. Hayden and E. J. Mele, *ibid.* **36**, 5010 (1987); A. J. Heeger, S. Kirelson, J. R. Schrieffer, and W. P. Su, Rev. Mod. Phys. **60**, 781 (1988).

¹³J. Yu and W. P. Su, Phys. Rev. B **44**, 13 315 (1991); Jinming Dong *et al.*, *ibid.* **52**, 9066 (1995).

¹⁴R. L. Fu, R. T. Fu, and X. Sun, Phys. Rev. B **48**, 17 615 (1993).

¹⁵R. Saito *et al.*, Phys. Rev. B **46**, 1804 (1992).